# **FRONTIER**

# Allylic C–H Functionalization via Group 9 $\pi$ -allyl Intermediates

Taylor A. F. Nelson,<sup>†,a</sup> Michael R. Hollerbach,<sup>†,a</sup> and Simon B. Blakey \*a

Received 00th January 20xx, Accepted 00th January 20xx

DOI: 10.1039/x0xx00000x

Allylic C–H functionalization catalysed by group 9 Cp\* transition-metal complexes has recently gained significant attention. These reactions have expanded allylic C–H functionalization to include di- and trisubstituted olefins, and a broad range of coupling partners. More specifically, several catalytic C–N, C–O, and C–C bond forming allylic C–H functionalization reactions have been reported, proceeding via MCp\*- $\pi$ -allyl intermediates. Herein we present an overview of these reactions by mechanistic paradigm. We also place this information in context of recent advances, as well as, limitations that remain for this class of reactions.

#### Introduction:

Transition-metal catalysed allylic substitution is recognized as a strategically powerful reaction for the synthesis of biologically relevant natural products, and drug candidates. Originally disclosed by Tsuji and Trost, 2,3 transition-metal catalysed allylic substitution proceeds via an organometallic  $\pi$ -allyl intermediate generated from an olefin with an allylic leaving group (Figure 1A). Allylic substitution reactions have been well studied and offer powerful control of regio- and enantioselectivity. Recent advances have provided allenes, alkynes, and dienes as alternative entry points to  $\pi$ -allyl intermediates, expanding the scope of electrophiles. Arguably, a more direct method to form a  $\pi$ -allyl intermediate is through activation of an allylic C–H bond

Despite early observations of stoichiometric allylic C–H functionalization, catalytic reactions remained elusive.<sup>7-9</sup> It was not until 2004, when White and co-workers reported a new Pd-catalyst system for allylic C–H acetoxylation, that

Figure 1. Development of Pd-Catalysed Allylic C–H Functionalization.

## A) Allylic Substitution (Tsuji-Trost Reaction)

#### B) Catalytic Palladium Allylic C-H Functionalization (White 2004-pres)

Electronic Supplementary Information (ESI) available: [details of any supplementary information available should be included here]. See DOI: 10.1039/x0xx00000x

allylic C–H functionalization was recognized as a viable reaction for complex molecule synthesis (Figure 1B). <sup>10</sup> This report paved the way for a number of important developments, including regio- and enantiocontrolled methods. <sup>9, 11</sup> Despite these significant advances, many challenges remain. The Pd-catalysed transformations are typically limited to terminal olefins and in most intermolecular cases provide the linear product. <sup>9</sup> Additionally, these reactions require soft nucleophiles such as malonates, and amines with two activating groups. These limitations have inspired new approaches to allylic C–H functionalization. This article focuses on the recent development and remaining challenges of group 9 Cp\* catalysed allylic C–H functionalization reactions, which provide complementary reaction profiles to those previously observed with palladium.

## **Discussion**

# 1st Generation Group 9-catalysed Allylic C–H Functionalization Reactions – Reactions promoted by an external oxidant:

In 2012, Cossy and co-workers disclosed an intramolecular allylic C–H amination utilizing [RhCp\*(MeCN)<sub>3</sub>](SbF<sub>6</sub>)<sub>2</sub> as a precatalyst.<sup>12</sup> The reaction was proposed to proceed via a RhCp\*-π-allyl intermediate and a Rh(III/I) catalytic cycle. However, no stoichiometric investigations or other mechanistic studies were performed to confirm this hypothesis. Notable advances in their investigation include the use of a Rh(III) catalyst, the use of alkylamine nucleophiles bearing only one activating electron-withdrawing group, and the observation that an internal olefin was reactive (Figure 2A). In the case of the internal allylic C–H activation of olefin 1, a 1:1 mixture of pyrrolidine 2 and piperidine 3 was observed in 50% combined yield (Figure 2A), demonstrating a lack of selectivity in the presumptive C–H activation step.

Supporting Cossy's hypothesis that these reactions proceed via  $\pi$ -allyl intermediates, the Tanaka group disclosed stoichiometric isolation and reactivity of RhCp<sup>E</sup>- $\pi$ -allyl complexes (Figure 2B, Cp<sup>E</sup> = 1,3-diethylester-2,4,5-

<sup>&</sup>lt;sup>a.</sup> Department of Chemistry, Emory University, Atlanta, Georgia 30322, United States.

<sup>†</sup> These authors contributed equally.

ARTICLE Journal Name

**Figure 2.** Foundational Work Establishing Rh-Catalysed Allylic C–H Functionalization

#### A) Rhodium Catalyzed Allylic C-H Amination (Cossy 2012)

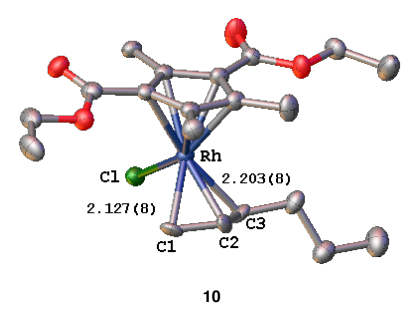
#### B) Stepwise Stoichiometric Rhodium Allylic C-H Amination (Tanaka 2016)

#### C) Formation of RhCpE-π-allyl Complexes from Internal Olefins (Tanaka 2016)

#### D) Stoichiometric Formation of Complex 10

$$[Cp^{\mathsf{E}\mathsf{RhCl}_2}]_2 \quad + \quad \begin{matrix} \mathsf{AgBF_4} \\ \mathsf{CsOAc} \\ \mathsf{DCM}, \, \mathsf{rt}, \, \mathsf{3h} \\ \mathsf{brine} \, \, \mathsf{quench} \end{matrix} \qquad \begin{matrix} \mathsf{EtO_2C} \\ \mathsf{Me} \\ \mathsf{Me} \\ \mathsf{Me} \\ \mathsf{Me} \end{matrix} \qquad \begin{matrix} \mathsf{Me} \\ \mathsf{Co2Et} \\ \mathsf{Me} \\ \mathsf{Me} \\ \mathsf{Me} \end{matrix} \qquad \begin{matrix} \mathsf{Me} \\ \mathsf{Co2Et} \\ \mathsf{Ne} \\ \mathsf{Me} \\ \mathsf{Me} \end{matrix} \qquad \begin{matrix} \mathsf{Me} \\ \mathsf{Co2Et} \\ \mathsf{Ne} \\ \mathsf{Me} \\ \mathsf{Me} \end{matrix} \qquad \begin{matrix} \mathsf{Me} \\ \mathsf{Ne} \\ \mathsf{Me} \\ \mathsf{Me} \\ \mathsf{Me} \\ \mathsf{Me} \\ \mathsf{Ne} \\ \mathsf$$

# E) Crystal Structure of RhCp $^{\text{E}}$ - $\pi$ -allyl Complex 10



trimethylcyclopentadiene).<sup>13</sup> Synthesis of RhCp<sup>E</sup>(III)-π-allyl complex **4** under catalytically relevant conditions brought the previously hypothesized Rh(III/I) catalytic cycle into question, as this intermediate did not undergo C–N bond formation. However, when complex **4** was reacted with AgSbF<sub>6</sub> as a halide scavenger, and Cu(OAc)<sub>2</sub> as an oxidant, amine **5** was isolated in 51% yield. Interestingly, when internal olefin **6** was subjected to the C–H functionalization conditions, three distinct Rh-π-allyl complexes were obtained (Figure 2C). Analysis of the reaction

mixture elucidated clear regioselectivity for internal π-allyl formation (8) over the corresponding terminal complex (7). Using analogous conditions, the authors were able to isolate complex 10 in 95% yield from 1-hexene and characterized the terminal π-allyl complex by single crystal x-ray diffractometry (SC-XRD, Figure 2D,E). Unsurprisingly, differing bond lengths were reported for Rh-C1 at (2.127(8) Å) and Rh-C3 (2.203(8) Å). This work provided an exemplary method to synthesize novel MCp<sup>E</sup>-π-allyl complexes from feedstock olefins. The investigations disclosed by Cossy and Tanaka provided a foundational platform that suggested intermolecular allylic C–H functionalization of internal olefins with a range of amine nucleophiles was feasible.

Subsequently, allylic C-H amination of internal olefins was investigated utilizing [RhCp\*Cl<sub>2</sub>]<sub>2</sub> as a precatalyst by Blakey and co-workers (Figure 3, 11-15).14 This investigation provided the first intermolecular allylic C-H amination of internal olefins, overcoming previous limitations of Pd-catalysis. A range of alkyl- and arylamines bearing only one activating electronwithdrawing group were effective, allowing for a variety of substituents to be present on the nucleophile, including amino acids (Figure 3, 12). Electron-rich styrenyl derivatives afforded up to 20:1 regioselectivity (14). In contrast, electron-deficient derivatives provided more modest 4:1 regioselectivity for the conjugated isomer (15). Deuterium exchange reactions supported a mechanism that was initiated by irreversible C-H cleavage. More recently, Jeganmohan and co-workers disclosed an analogous follow-up study, in which IrCp\* was used as the catalyst.15

To further understand the potential of these group 9 Cp\* complexes to catalyse allylic C–H functionalization, Blakey and co-workers investigated the Rh-catalysed allylic C–H etherification of internal olefins utilizing simple alcohols as the oxygen coupling partner (Figure 4, 16-20). Most notably, there was limited competitive oxidation of the alcohol coupling partner to the aldehyde or overoxidation of the ether product. Wide functionality was tolerated for the olefin and alcohol coupling partners, including complex molecules, such as sugars,

Figure 3. Allylic C-H Amination of Internal Olefins (Blakey 2017)

 $<sup>^</sup>a$  Reactions were performed in DCM at 40  $^o$ C for 24 h.  $^b$  Reactions were performed in DCE at 60  $^o$ C for 48 h.  $^c$  Reactions were performed in DCE at 80  $^o$ C for 48 h.  $^d$  Reactions were performed in DCE at 65  $^o$ C for 8 h.

Journal Name ARTICLE

Figure 4. Allylic C-H Etherification of Internal Olefins (Blakey 2018)

$$\begin{array}{c} & \begin{array}{c} & \begin{array}{c} R_3 O H \ (5\text{-}10 \ equiv) \\ [RhCp^*Cl_2]_2 \ (2 \ mol\%) \\ AgSbF_6 \ (10 \ mol\%) \\ \end{array} \\ & \begin{array}{c} AgOAc \ (2.2 \ equiv) \end{array} \\ \end{array} \\ \begin{array}{c} \begin{array}{c} P_1 \\ \\ \end{array} \\ \end{array} \\ \begin{array}{c} P_2 \\ \end{array} \\ \begin{array}{c} \begin{array}{c} P_3 \\ \\ \end{array} \\ \end{array} \\ \begin{array}{c} P_4 \\ \end{array} \\ \begin{array}{c} OTBDPS \\ \end{array} \\ \begin{array}{c} 17, \ R = H, 87\%^b \\ 18, \ R = OMe, 58\%^c \\ \end{array} \\ \begin{array}{c} 16, 56\%^a \\ \end{array} \\ \begin{array}{c} 16, 56\%^a \\ \end{array} \\ \begin{array}{c} 19, \ R = CF_3, 45\%^d \\ \end{array} \\ \begin{array}{c} 0 \\ \end{array} \\ \begin{array}{c} P_1 \\ \end{array} \\ \begin{array}{c} P_2 \\ \end{array} \\ \begin{array}{c} OTBDPS \\ \end{array} \\ \begin{array}{c} OTBD$$

 $^{\rm a}$  Reactions were performed in DCE at 60 °C for 24 h.  $^{\rm b}$  Reactions were performed with 5 mol% [RhCp\*Cl $_{\rm 2}$ ] $_{\rm 2}$  in DCE at 60 °C for 5 h.  $^{\rm c}$  Reactions were performed in DCE at 60 °C for 4 h.  $^{\rm d}$  Reactions were performed with 5 mol% [RhCp\*Cl $_{\rm 2}$ ] $_{\rm 2}$  in DCE at 60 °C for 48 h.  $^{\rm e}$  Reactions were performed in DCE at 60 °C for 48 h.

steroids, and amino acids (20). In all cases, the reaction was regioselective for the conjugated product and good to excellent yields were obtained. Mechanistic studies detected no deuterium scrambling, when deuterated olefin (3-d<sub>2</sub>-1,3-diphenylpropene) was used as the olefin, again indicating irreversible C–H activation. Additionally, kinetic isotope effects suggested that C–H cleavage was the rate determining step.

Concurrently, Glorius and co-workers reported a Rhcatalysed cross-dehydrogenative allylic C-H heteroarylation.<sup>17</sup> Notably, the key C-C bond forming reaction showed no competitive heck coupling (Figure 5). Thiophenes, arylated at the 5-position, were chosen as the coupling partner to prevent further reactivity with a second equivalent of olefin. Substituted thiophenes were utilized with a variety of terminal and internal olefins resulting in moderate to excellent yields (21-23). Additional electron-rich heterocycles also performed well including, furans, benzofurans, pyrroles, and indoles (22). Furthermore, stoichiometric formation of RhCp\*-π-allyl complex 24 was described, with complex 24 obtained in 10% isolated yield (Figure 6). The authors reported a SC-XRD structure with similar bond distances to those observed by Tanaka at Rh-C1 (2.168(5)Å) and Rh-C3 (2.218(5)Å). Notably, the methyl of the Cp\* ring sits above the middle C2 carbon at 2.7(5)°, whereas the opposite is true when the Cp<sup>E</sup> ligand was employed for Tanaka (Figure 6). Complex 24 was subjected to catalytically relevant conditions, resulting in 24% yield of

Figure 5. Allylic C-H Heteroarylation (Glorius 2018)

Figure 6. Stoichiometric  $\pi$ -allyl Complex Synthesis and Reactivity (Glorius 2018)

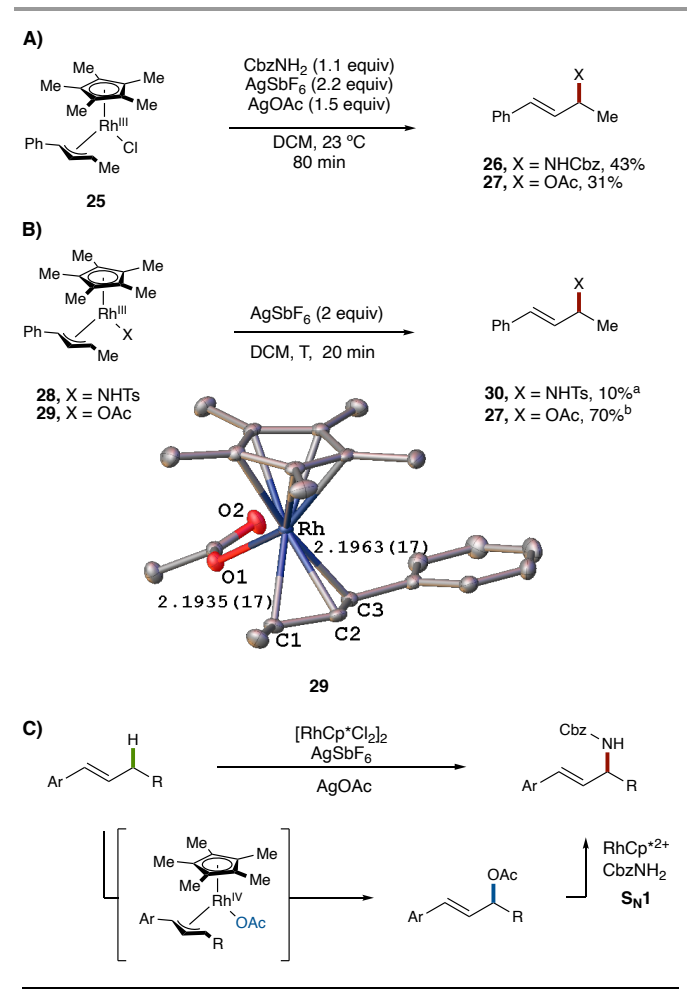
expected allyl product 23 (Figure 6). While the stoichiometric studies were in agreement with  $\pi$ -allyl complex formation, they did not afford a complete mechanistic picture.

In order to further develop these reactions, Blakey, Baik, and MacBeth undertook a full mechanistic investigation of the allylic amination protocol. 18 Kinetic analysis seminal demonstrated that as expected, the reaction was 1st order in Rh and olefin, and also indicated that the reaction was inhibited by the amine nucleophile. KIE data supported C-H cleavage as the rate-determining step. For this reason, overall kinetic analyses could not provide insight into the key bond-forming step. To determine plausible intermediates in the catalytic cycle, RhCp\*- $\pi$ -allyl complexes 25, 28, and 29 were synthesized and characterized by SC-XRD (Figure 7). Overall bond distances and angles were similar across the three complexes, but the shortest Rh-C bond distances were observed with complex 29, with a Rh-C1 bond distance of 2.1935(7) Å and Rh-C3 distance of 2.1963(17) Å. Complex 25 was subjected to catalytically relevant conditions resulting in allylic amine 26 in 43% yield, and allylic acetate 27 in 31% yield. Importantly, reactivity was not observed in the absence of a halide scavenger, oxidant, or acetate source. To test oxidatively induced reductive elimination as the bond forming process, complexes 28 and 29 were subjected to a Ag(I) oxidant. Oxidation of complex 28 resulted in only 10% yield of amine product 30, while oxidation of complex 29 resulted in facile conversion to allylic acetate 27 in 70% yield. The low yield in the direct conversion to the amine product 30 was not consistent with 28 as an intermediate in the catalytic cycle. However, the high yield of acetate 27, suggested that an allylic acetate may be a relevant intermediate.

Moreover, cyclic voltammetry and computational analyses were performed, and supported the conclusion that oxidatively induced reductive elimination of complex **29** affords allylic acetate **27**, proceeding through a Rh(IV) intermediate. Consequently, Lewis acid-mediated allylic substitution (S<sub>N</sub>1) of acetate **27** to amine **30** (Figure 7b) via a RhCp\*<sup>2+</sup> catalyst was confirmed by computational and experimental investigations. Overall, a Rh(III)/Rh(IV)/Rh(II)/Rh(III) catalytic cycle was

ARTICLE Journal Name

Figure 7. Stoichiometric Mechanistic Investigations



 $^{\rm a}$  AgSbF $_{\rm 6}$  (2 equiv), NH<sub>2</sub>SO<sub>2</sub>Ph (2 equiv), DCM, 40 °C. 10% combined yield of NHTs and NHSO<sub>2</sub>Ph products (1:1.5).  $^{\rm b}$  CD<sub>2</sub>Cl<sub>2</sub> used instead of DCM at 25 °C.

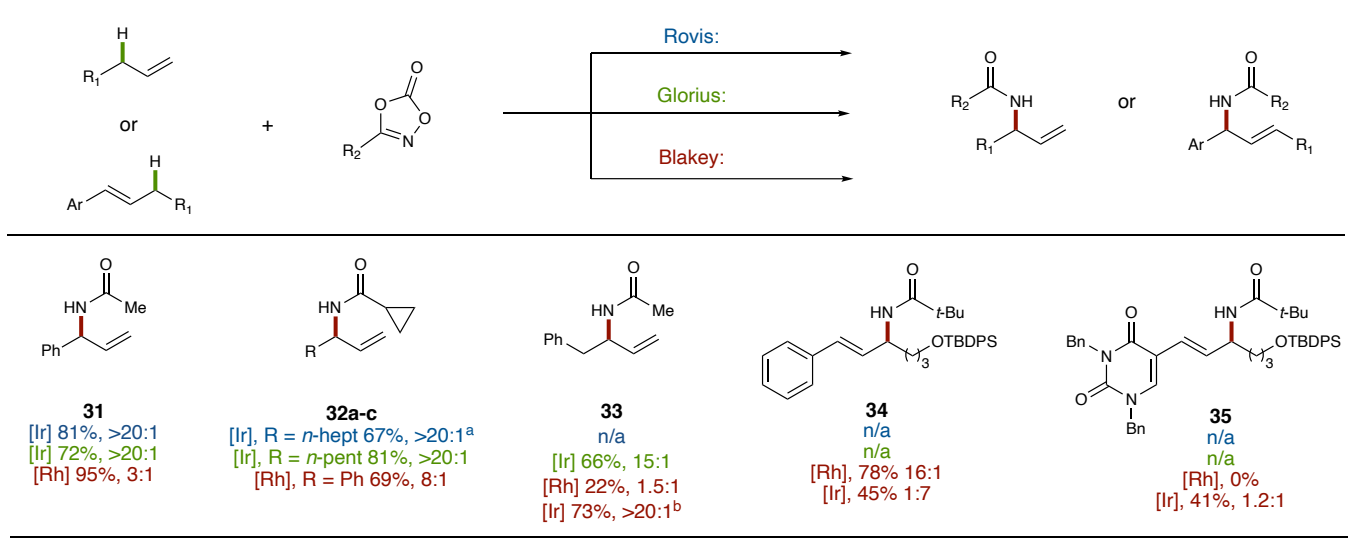
Figure 8. Allylic C-H Amidation via Dioxazolone Nitrenoid Precursors

proposed to form the allylic acetate, followed by rapid conversion to the amine product via an off-cycle Lewis acid-catalysed substitution (Figure 7C). Retrospectively, the allylic etherification<sup>16</sup> and heteroarylation<sup>17</sup> reports are consistent with this mechanistic paradigm.

# $2^{nd}$ Generation Group 9-catalysed Allylic C–H Functionalization Reactions – Reactions proceeding via direct reductive elimination from M(V) metallonitrene intermediates:

While the first-generation group 9-catalysed allylic C–H functionalization protocols did provide novel reactivity engaging internal olefins, off-cycle S<sub>N</sub>1 substitution limited control of bond formation at the metal center. Regiodivergent and enantioselective approaches would be required for widespread adoption of this methodology. Consequently, methods that allowed direct reductive elimination of the desired C–X bond were required to allow for catalyst-controlled induction of regio-and enantioselectivity. To this end, nitrene precursors were proposed as excellent candidates for the direct reductive elimination of the desired allylic product via an oxidatively induced M(III)/(V) mechanism. As a testament to the importance of leveraging a second mechanistic pathway, several groups have reported C–N bond forming methodologies utilizing M(V) nitrenoid intermediates.

In quick succession, Rovis,<sup>19</sup> Glorius,<sup>20</sup> and Blakey<sup>21</sup> disclosed allylic C–H amidation protocols utilizing dioxazolone nitrenoid precursors. (Figure 8). Contrary to previous allylic C–H functionalization methods, these procedures were selective for the branched/benzylic amidation product. While analogous, all groups developed distinct conditions with subtle nuances in halide scavenger and carboxylate sources. Rovis and Glorius optimized to similar conditions with an IrCp\* precatalyst focusing on terminal olefins. Similarly, Blakey and co-workers developed RhCp\* or IrCp\* catalysed systems for mono-, di-, and trisubstituted olefins. A broad range of dioxazolone coupling



Rovis Conditions: Dioxazolone (1.2 equiv), [IrCp\*Cl $_2$ ] (2.5 mol%),AgNTf $_2$  (15 mol%). LiOAc (20 mol%), DCE, 35 °C, 20 h; Glorius Conditions: Dioxazolone (1.5 equiv), [IrCp\*Cl $_2$ ] (2 mol%), AgSbF $_6$  (10 mol%), AgOAc (10 mol%), DCM, 40 °C, 18 h; Blakey Conditions: Dioxazolone (2.0 equiv), [IrCp\*Cl $_2$ ] (2.5 mol%) or [RhCp\*(MeCN) $_3$ ](SbF $_6$ ) (5 mol%), AgSbF $_6$  (30 mol%), CsOAc (5 mol%), DCE, 40 °C, 24 h

<sup>a</sup> Reactions were performed at 60 °C. <sup>b</sup> 40 mol% AgSbF<sub>6</sub> was used.

Journal Name ARTICLE

partners were tolerated across the three disclosures, providing biologically relevant amide functionality. Collectively, the three reports revealed that distinct reactivity was directly correlated to the MCp\* precatalyst. With unactivated terminal olefins, IrCp\* provided optimal yields and greater selectivity for the branched isomer compared to the analogous RhCp\* (31-33). On the contrary, RhCp\* afforded increased yield and selectivity for the benzylic isomer with internal olefins, while IrCp\* favored the conjugated isomer (34,35).

In an attempt to understand the origins of the strikingly different regioselectivities observed between the RhCp\* and IrCp\* catalysed reactions, stoichiometric studies were undertaken. RhCp\*- and IrCp\*-π-allyl chloro complexes 25 and **36** were isolated and characterized by SC-XRD (Figure 9).<sup>21</sup> For complex 25 the Rh-C1 bond was 2.2008(7) Å, while the Rh-C3 bond was 2.2235(7) Å. As was expected for the iridium complex, the Ir-C bonds were slightly shorter with Ir-C1 at 2.1811(19) Å and Ir-C3 at 2.2095(17) Å. However, in both complexes the benzylic M-C3 bond was longer than the distal M-C1 bond, thus offering no obvious structural basis for the observed divergent regioselectivities. When complexes 25, 36 were subjected to dioxazolone 37 and a halide scavenger, amides 38-39 were formed in comparable yields and regioselectivities to the catalytic conditions (Figure 9). These results support the hypothesis that the  $\pi$ -allyl complex is an intermediate in the reaction, and that subsequent engagement of the dioxazolone and nitrene formation leads to an inner-sphere reductive elimination to form the product. While detailed experimental and computational mechanistic investigations are still ongoing, a M(III)/M(V) cycle is likely.

Further investigations were performed utilizing tosylazides as the nitrenoid precursor. Blakey and co-workers have disclosed

Figure 9. Stochiometric  $\pi$ -allyl Complex Structure Comparison and Reactivity

an IrCp\* catalysed branched selective protocol, focusing on allylbenzene derivatives. The use of fluorinated alcohol solvents was required in these reactions, with hexafluoroisopropanol (HFIP) providing optimal yields. Rovis and co-workers have performed further studies with unactivated 1,1-and 1,2-disubstuted olefins and demonstrated impressive regioselectivity, dependent on mild electronic differences of the C–H bonds and appropriate catalyst and ligand choice. A strong correlation between 1JCH coupling constants and activation barriers was observed and offers significant predictive value.

# Allylic Functionalization Reactions for Which the Mechanism Remains Unclear:

The reports described above have fallen into two mechanistic categories, either proceeding via a M(IV) or M(V) oxidation state. Despite the similarities of prior work, some reports of allylic C-H functionalization via  $\pi$ -allyl complexes do not obviously correspond to either elucidated mechanistic hypotheses. Glorius and co-workers reported allylic C-H arylation reactions using arylboroxine coupling agents and AgOAc as the terminal oxidant (Figure 10).24 A variety of arylboroxine reagents were utilized to provide allylic products in good to excellent yield (40-42). Tentatively, the authors propose transmetallation of the boron reagent onto a  $\pi$ -allyl complex followed by reductive elimination (Rh(III)-Rh(I)). The mechanistic studies do not provide a clear picture with which to determine discrete intermediates. Furthermore, deuterium scrambling and KIE studies support a non-rate limiting, irreversible C-H activation, in stark contrast with previous reports.<sup>16, 18</sup> While the current mechanism is unknown, the need to expand C-H allylic functionalization towards new C-C bond forming reactions is crucial for the application to complex molecule synthesis.

Additionally, an intriguing RhCp\* catalysed cyclization with subsequent allylic C–H functionalization providing complex indole products was reported by Li and co-workers (Figure 11, **46-48**).<sup>25</sup> The authors proposed that alkyne **43** cyclizes to form Rh-indole intermediate **44**, followed by  $\pi$ -allyl complex formation and reductive elimination to afford indole **45** in good yield. While this chemistry appeared to be related to the heteroarylation performed by Glorius and co-workers (Figure 5),<sup>17</sup> the free indole was not found to be a competent nucleophile. Similarly, no competitive allylic amination was observed, and non-productive protodemetallation of complex **44** was

Figure 10. Allylic C-H Arylation with Arylboroxine Reagents

This journal is © The Royal Society of Chemistry 20xx

ARTICLE Journal Name

Figure 11. Allylic C-H Indolylation via Cyclization

minimized under optimized conditions. Deuterium exchange was not observed and control experiments support  $\pi$ -allyl complex formation. Through complete mechanistic understanding of these uncategorized reactions, we foresee the ability to broaden the scope of C–C bond formation via allylic C–H functionalization.

#### **Conclusions and Outlook:**

Allylic C-H functionalization proceeding via a  $\pi$ -allyl intermediate has been advanced by the introduction of group 9metal-catalysed systems. After pivotal intramolecular disclosures, intermolecular Rh-catalysed C-N, C-O, and C-C bond forming reactions, as well as an Ir-catalysed amination, were developed. Mechanistic investigations of the seminal amination work, focused on putative organometallic intermediates, and supported a Rh(III)/(IV)/(II)/(III) catalytic cycle. It was discovered that direct reductive elimination of an allylic acetate from the Rh(IV)- $\pi$ -allyl intermediate, followed by Lewis acid-mediated substitution, provided the aforementioned products. Focus was then shifted to developing a complementary method to afford direct reductive elimination of the desired product from the discrete metal- $\pi$ -allyl intermediate. In short succession, several methods were disclosed proceeding through a M(III)/(V) pathway with the use of nitrenoid precursors. These second-generation methods provided complementary regioselectivity to the first-generation disclosures. Additional investigations for allylic arylations may afford a third mechanistic category altogether.

This work has been disclosed in a relatively short time frame and requires further investigations to realize the full synthetic utility in complex systems. Foundational work with organometallic species has proven crucial for the reports discussed and will provide useful mechanistic insight for future disclosures. The development of enantioselective methods is the next logical frontier for allylic C–H functionalization, and the second-generation reactions offer significant promise for further development. Additionally, we note that while these transformations have been expanded to tolerate a wide array of olefins, limitations remain, including cis-disubstituted, tetrasubstituted, and cyclic olefins. Furthermore, the impact of

functionality in close proximity to the  $\pi$ -allyl complex has not yet been systematically explored. Regardless of the next breakthrough in this field, group 9-catalysed intermolecular allylic C–H functionalization is no longer a  $\pi$ -in-the-sky idea and has proven to be a simple, atom economical method to access allylic products.

#### **Conflicts of interest**

There are no conflicts to declare.

### **Acknowledgements**

This work was supported by the National Science Foundation (NSF) under the CCI Center for Selective C–H Functionalization (CHE-1700982). T.A.F.N was partially supported by the American Chemical Society Petroleum Research Fund (ACS-PRF-59563-ND1).

#### References

- G. Helmchen, M. Ernst and G. Paradies, *Pure Appl. Chem.*, 2004, **76**, 495-505.
- J. Tsuji, H. Takahashi and M. Morikawa, *Tetrahedron Lett.*, 1965, 6, 4387-4388.
- B. M. Trost and T. J. Fullerton, J. Am. Chem. Soc., 1973, 95, 292-294.
- U. Kazmaier, Transition metal catalyzed enantioselective allylic substitution in organic synthesis, Springer Science & Business Media, 2011.
- P. Koschker and B. Breit, Acc. Chem. Res., 2016, 49, 1524-1536.
- X.-H. Yang and V. M. Dong, J. Am. Chem. Soc., 2017, 139, 1774-1777.
- 7. R. Hüttel and J. Kratzer, *Angew. Chem.*, 1959, **71**, 456-456.
- R. Hüttel and M. Bechter, Angew. Chem., 1959, 71, 456-456
- F. Liron, J. Oble, M. M. Lorion and G. Poli, Eur. J. Org. Chem., 2014, 2014, 5863-5883.
- M. S. Chen and M. C. White, J. Am. Chem. Soc., 2004, 126, 1346-1347.
- 11. R. Wang, Y. Luan and M. Ye, *Chin. J. Chem*, 2019, **37**, 720-
- T. Cochet, V. Bellosta, D. Roche, J.-Y. Ortholand, A. Greiner and J. Cossy, Chem. Commun., 2012, 48, 10745-10747.
- 13. Y. Shibata, E. Kudo, H. Sugiyama, H. Uekusa and K. Tanaka, *Organometallics*, 2016, **35**, 1547-1552.
- 14. J. S. Burman and S. B. Blakey, *Angew. Chem. Int. Ed.*, 2017, **56**, 13666-13669.
- P. Sihag and M. Jeganmohan, J. Org. Chem., 2019, 84, 13053-13064.
- T. A. F. Nelson and S. B. Blakey, Angew. Chem. Int. Ed., 2018, 57, 14911-14915.
- A. Lerchen, T. Knecht, M. Koy, J. B. Ernst, K. Bergander, C.
  G. Daniliuc and F. Glorius, Angew. Chem. Int. Ed., 2018, 57, 15248-15252.

Journal Name ARTICLE

- R. J. Harris, J. Park, T. A. F. Nelson, N. Iqbal, D. C. Salgueiro,
  J. Bacsa, C. E. MacBeth, M. H. Baik and S. B. Blakey, *J. Am. Chem. Soc.*, 2020, 142, 5842-5851.
- H. Lei and T. Rovis, J. Am. Chem. Soc., 2019, 141, 2268-2273.
- 20. T. Knecht, S. Mondal, J. H. Ye, M. Das and F. Glorius, *Angew. Chem. Int. Ed.*, 2019, **58**, 7117-7121.
- J. S. Burman, R. J. Harris, C. M. B. Farr, J. Bacsa and S. B. Blakey, ACS Catal., 2019, 9, 5474-5479.
- A. M. Kazerouni, T. A. F. Nelson, S. W. Chen, K. R. Sharp and
  S. B. Blakey, J. Org. Chem., 2019, 84, 13179-13185.
- 23. H. Lei and T. Rovis, *Nat. Chem.*, 2020, DOI: 10.1038/s41557-020-0470-z.
- T. Knecht, T. Pinkert, T. Dalton, A. Lerchen and F. Glorius, ACS Catal., 2019, 9, 1253-1257.
- J. Sun, K. Wang, P. Wang, G. Zheng and X. Li, Org. Lett., 2019, 21, 4662-4666.